J. Fluid Mech. (1993), *vol.* 249, *pp.* 521–534

Investigation of the fractal structure of jets and plumes

By G. F. LANE-SERFF

Department of Oceanography, The University, Highfield, Southampton, SO9 5NH, UK

(Received 17 February 1992 and in revised form 14 October 1992)

This paper is a description of an experimental study of round, turbulent jets and plumes, investigating the effects of buoyancy on the fractal structure. The jets and plumes are formed by injecting fluid from a small source, with diameter, d, of 0.508 mm, into a stationary body of water contained in a tall tank of dimensions 1.75 m high by 0.6 m by 0.6 m. For both jets and plumes the Reynolds number at the source was in the range 800 to 1800, and the flow was observed in the far field at distances $250d$ to $550d$. In the case of the plumes momentum still dominated near the source so that the flow was fully turbulent before buoyancy forces had a significant effect. The source fluid was dyed with fluorescein, and the flow was illuminated by a 'thick' sheet of light (thick in the sense of many Kolmogorov scales) effectively giving a projection rather than a true two-dimensional slice. The fractal dimensions of contours of concentration on this projection were measured, with care taken to normalize with respect to the local intensity and lengthscales. There were no significant differences in the results for jets and plumes, so the smaller scales of motion seem unaffected by the presence of buoyancy forces. The fractal dimension was found to be a function of threshold intensity, with an apparent minimum of 1.23. This may be an artefact of the noise level, however, and an estimated value for the zero-intensity threshold of 1.16 may be important, though the use of a single value for the fractal dimension is questionable. The implications of the results for measurements where no account has been taken of local scales is discussed.

1. Introduction

This paper describes the results of an experimental study of round, turbulent jets and plumes. Plumes occur where fluid of different density from the ambient fluid is injected (such as smoke rising from a chimney), jets occur where the injected fluid has the same density as the ambient fluid. In this paper the initial flow is directed vertically and in the same direction as the buoyancy forces. On entering the ambient fluid the source fluid flow becomes unstable (see, for example, Crow & Champagne 1971) so that after ten to twenty source diameters the flow is turbulent, engulfing ambient fluid.

The purpose of this study was to investigate the structure of the instantaneous boundary between the turbulent jet or plume fluid and the ambient fluid, in particular to study the influence of buoyancy forces on a turbulent flow. There is a clear difference between the energy balances in a jet flow, where the only source of energy is the kinetic energy at the source, and in plume flow, where there is a continuous release of potential energy throughout the flow. A general review of energy dissipation is given by Kotsovinos (1990). Here I will just give a brief outline of some energy considerations. Consider a simple mean flow model based on the entrainment assumption as described by Morton, Taylor & Turner (1956). In this model the plume

or jet is treated as a straight-sided cone, with entrainment of ambient fluid into the cone at a speed proportional to the mean centreline speed. The constant of proportionality (the 'entrainment constant', generally denoted by α) may be different for jets and plumes (α_J and α_P say). Writing R for the radius, Z for the distance from the source and U for the mean speed, this model gives R proportional to Z for both jets and plumes ($R = 2\alpha_J Z$ for jets and $6\alpha_P Z/5$ for plumes) with $U \propto 1/R$ for jets and $U \propto 1/R^{\frac{1}{3}}$ for plumes. The rate of loss of kinetic energy in the jet flow is $\alpha_J U^3/R$ per unit mass. For the plume flow there is an increase in kinetic energy of $\frac{3}{5}\alpha_P U^3/R$, but this is less than the release of potential energy, which is $\frac{8}{5}\alpha_P U^3/R$. Thus the energy dissipation is $\alpha_J U^3/R$ for jets and $\alpha_P U^3/R$ for plumes. Apart from the possible difference between α_J and α_P, the dependence of the dissipation rate on the local velocity and length scales is the same for both types of flow.

The flows were studied by measuring the fractal dimension of the boundary between the turbulent plume or jet fluid and the ambient fluid. In many practical situations it is necessary to know the effective area (measured at an appropriate small scale) of contact between a contaminant plume and the ambient in order to calculate the rate of diffusion or chemical reaction between the plume and its environment. If the fractal dimension and the inner cutoff scale are known then the area of the interface can be calculated. The fractal dimension also gives information about the flow similar to that traditionally obtained by power spectra and correlations (Hunt & Vassilicos 1991). However, a smaller range of scales is needed to satisfactorily define a fractal dimension than is needed for a conventional power spectrum, and flows with lower Reynolds number than would normally be considered fully turbulent give 'high Reynolds number' fractal dimensions. The fact that a smaller range of scales is needed is useful in experiments, where the resolution of the measurements may only give a limited range of scales, and for numerical models, which may only have a limited range of scales and also a fairly low effective Reynolds number.

Important parameters in considering jet and plume flows are the specific fluxes of momentum and buoyancy at the source. These are given by

$$M_T = \int u^2 \, \mathrm{d}A \quad \text{and} \quad B_T = \int u g' \, \mathrm{d}A,$$

where u is the downstream velocity and g' is the 'reduced gravity' equal to $g(\Delta\rho/\rho)$, with ρ the ambient density and $\rho + \Delta\rho$ the density of the source fluid. From these a lengthscale can be calculated,

$$L_J = M_T^{\frac{3}{4}} B_T^{-\frac{1}{2}},$$

known as the 'jet length'. Near the source a plume flow behaves like a jet with buoyancy having a negligible effect. Further from the source, on the scale of the jet length, the buoyancy begins to dominate the flow. (Note that some authors use the above fluxes divided by π for convenience when dealing with circular sources, and their jet length differs by a factor of $\pi^{\frac{1}{4}}$.)

The apparent area of the convoluted boundary between the plume fluid and the ambient fluid increases as one measures at smaller and smaller scales. At scales between the large scale set by the flow (the plume width) and the small scale where viscosity becomes important (the Kolmogorov scale) one expects the dynamics to be scale-independent. Thus one expects the flow to be self-similar in this range with the flow appearing the same under a range of magnifications, so that the relationship between area and measuring scale would be of the form: area $= kL^2 L^{-D}$, where L is the measuring scale and D is known as the fractal dimension. If the interface were a cone

then $D = 2$ and the apparent area remains constant; if the interface were a space-filling sponge then $D = 3$ and the area would be inversely proportional to the measuring scale. A method of estimating the fractal dimension is to count the number of cubes, N, of size L needed to completely contain the surface. For a cone $N = kL^{-2}$, for the space-filling shape $N = kL^{-3}$, and for the interface at the edge of the plume a dimension between two and three is expected. Though the dimension estimated by box-counting methods is identical to the fractal dimension for many shapes, the relationship is not trivial (see, for example, Hunt & Vassilicos 1991). However, the term fractal dimension will be used in this paper for the measured dimensions, though they might more accurately be called 'box dimensions'. If a two-dimensional slice is taken through the surface then a line is obtained, and its dimension can be evaluated by considering the number of squares of a given size needed to contain the line. A true two-dimensional slice will give a line of dimension one less than the surface. In the experiments described here a 'thick' sheet of light (passing through the central axis of the jet or plume) is used, which results in a line of smaller dimension. In jet flows Prasad & Sreenivasan (1990) found that increasing the thickness of the slice decreased the dimension of the line from 1.36 to 1.22, with the limit reached once the sheet was more than about ten Kolmogorov scales thick. This value is the same as that obtained for a two-dimensional projection, which is not surprising since most of the contribution to a projection comes from the widest part of the flow. The relationship between the fractal dimension of the boundary of a projection of a fractal surface (as measured here) and the fractal dimension of that surface is not known. The projection boundary could be regarded as the set of 'outermost' points of a collection of planar cuts of the original surface. It seems likely that the length of this set of outermost points grows less rapidly with finer measuring scale than does the length of one cut, but there are no general results on this subject.

While jet flows have received much experimental attention, especially the flow near the source, flows where buoyancy is important have not been studied in such detail. (A comprehensive survey is given in a review paper by List 1982.) Even for jets, studies have largely been confined to statistical analyses of one- or two-point measurements with little consideration of large-scale structures.

A particularly thorough study of the statistical properties of jets and plumes is described by Papanicolaou & List (1988). They investigated plumes and jets with Reynolds number at the source of approximately 1000 for plumes and 5000 for jets, taking measurements up to 100 source diameters from the source. The jet length varied down to half a source diameter (for a pure jet the jet length may be regarded as infinite). Using a similar range of parameters Papantoniou & List (1989) investigated large-scale structure by measuring the concentration on a line perpendicular to the plume centreline over a time of several minutes. They identify large-scale features passing the measuring station and give the typical form of these features: a sharp increase in concentration at the 'front' of the feature, decaying more gradually at the 'rear'.

In the present work the far field of the flow (several hundred source diameters downstream) is observed. In addition (for plume flows) the jet length is always at least 50 source diameters so that the flow is fully turbulent before buoyancy has a significant effect. In the next section the experimental details are described and in §3 the image processing procedure used to analyse the experiments is set out. The results will be given in §4 and some discussion and conclusions in §5.

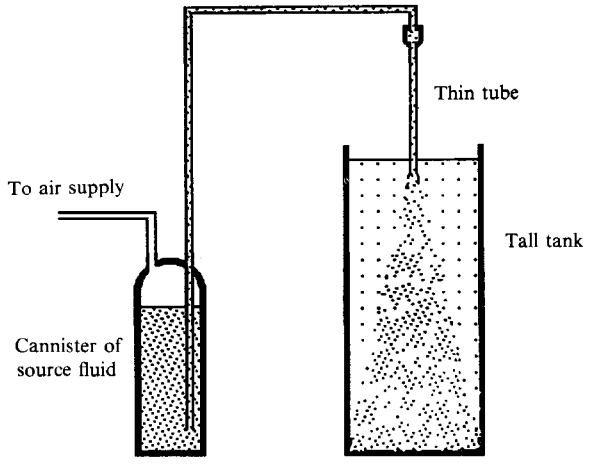

FIGURE 1. Schematic section of the apparatus.

2. Experiments

The experiments consisted of injecting source fluid vertically down into a large tank of water (60 cm square by 1.75 m high). The source was a 50 cm long tube of internal diameter 0.508 mm. The source fluid was forced through this tube from a pressurized canister at a pressure of about 50 p.s.i. (350 kPa). This gives a steady flow rate of up to 1 $cm^3 s^{-1}$. Density differences of up to 18% were produced by adding salt to the source solution. The source Reynolds numbers were in the range 800 to 1800 for both jets and plumes. In calculating the momentum flux it was assumed that the flow in the tube was Poiseuille. Plumes can be achieved with jet lengths down to 2 cm: note that this is still many times the source diameter so that turbulent flow is fully established before buoyancy forces begin to dominate. A sketch of the apparatus is given in figure 1.

The flow was visualized by adding fluorescein dye to the source fluid. The diffusivities of both the dye and salt are about 1000 times smaller then the viscosity of water, and the diffusive scales below the Kolmogorov scale will not be examined here. The flow was illuminated by a vertical light sheet from conventional slide projectors about 2 m from the tall tank. The light sheet was produced by masks on the side faces of the tall tank, having slits of adjustable width. With only one projector there is some attenuation in observed intensities between the part of the flow nearer the light source and that away from the source. This is due partly to the absorption of light by the dye and partly to the spreading of light from the source. These effects are greatly alleviated by the use of two projectors. (See figure 2.)

The light sheet was adjusted to taper to a point at the same (vertical) level as the source of injected fluid. The tapered sheet of light has two main advantages over a parallel-sided sheet. First, with any sheet of light one is effectively averaging the concentration over the thickness of the sheet. With a tapering sheet this averaging is performed over a thickness proportional to the local plume width whereas with a parallel-sided sheet the averaging is performed over smaller scales (compared with the local plume width) as one goes further from the source. Second, since the concentration of source fluid decreases with distance from the source, the intensity of light 'reflected' by the dye with a sheet of constant width also decreases. With a tapered sheet there is no decrease in mean intensity for a jet, and less decrease for a plume, as one goes

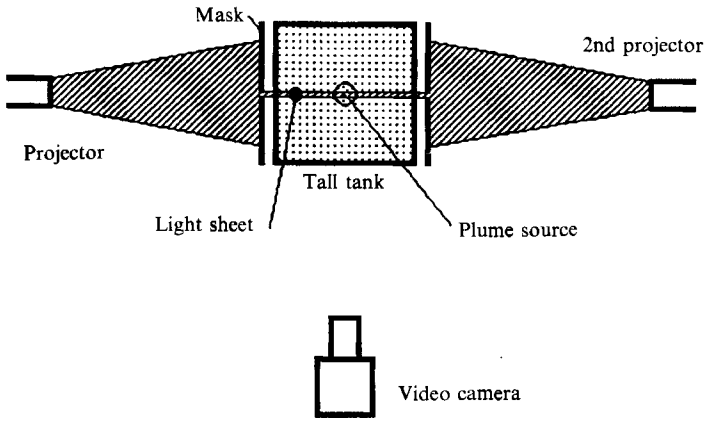

FIGURE 2. Schematic plan of the apparatus showing the lighting and video camera.

Experiment	Reynolds number $Re = ud/\nu$	Reduced gravity g' (cm s^{-2})	Jet length L_J (cm)	Symbol in figure 8
J1	1400	0	∞	+
J2	1700	0	∞	×
J3	1300	0	∞	□
J4	960	0	∞	○
P1	1300	45.1	12.6	*
P2	1800	45.1	18.3	✡
P3	1300	152	5.62	△
P4	1200	181	6.02	▽
P5	800	181	4.02	◇

TABLE 1. Values of the experimental parameters for experiments J1–J4 (jets) and P1–P5 (plumes)

further from the source. This gives much improved resolution of the concentration field far from the source.

In these experiments the Kolmogorov scale (the scale below which viscous effects dominate) was about 0.2 mm. It should be noted that the light sheet was always much thicker than the Kolmogorov scale. The flow was recorded by a high-quality video system.

The values of the experimental parameters are given in table 1. The Reynolds number given is that at the source, based on the source diameter and the mean velocity there. Note that the Reynolds number (*Re*) does not vary with distance from the source for jet flows (the mean jet speed is inversely proportional to the distance) but does increase for plume flows (but only significantly at distances greater than one jet length).

3. Image processing

The video recordings of the experiments were processed using a micro computer (PC/AT type) in conjunction with an S-VHS video recorder. Video images are digitized by a frame-grabber to give an array of values corresponding to the intensity of the light. The array was 512 by 512, with intensities recorded as integers in the range 0 to 255. Each pixel in the image represents an area in the flow of approximately 0.2 mm square (of the order of the Kolmogorov scale), with the whole imaged area

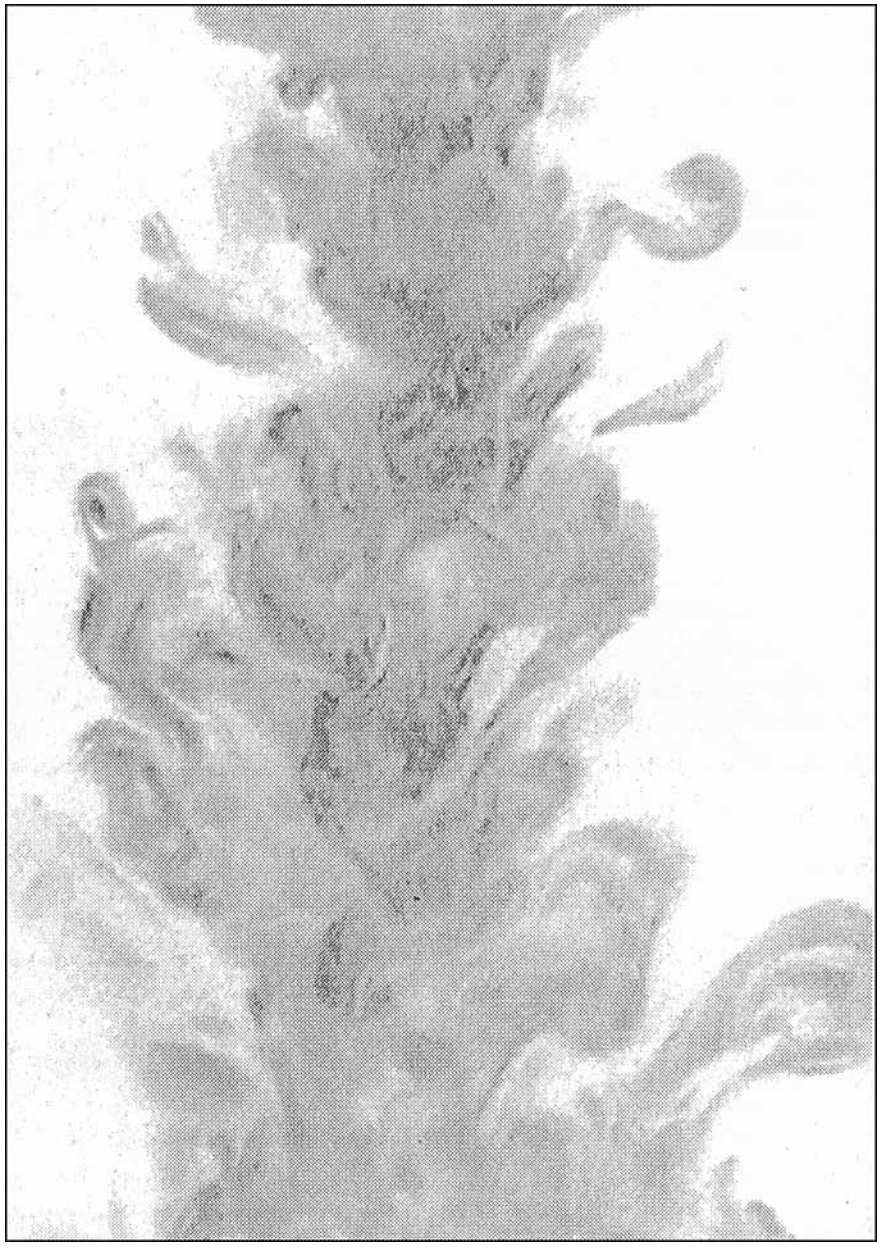

FIGURE 3. A digitized image from an experiment. The darker shades correspond to higher light intensities so this is essentially a negative of what is observed.

being approximately 100 mm square, centred 175 mm from the source. In calibration experiments it was found that the values given by this technique were related linearly to the dye concentration, at least for the relatively low light intensities used in these experiments (nonlinearities are apparent for higher intensities where the response flattens off). Figure 3 shows a digitized image from a single frame. For each experiment the mean intensities were found by taking an average of 250 video frames, taken at regular intervals from two minutes of recordings (thus about one frame every half-

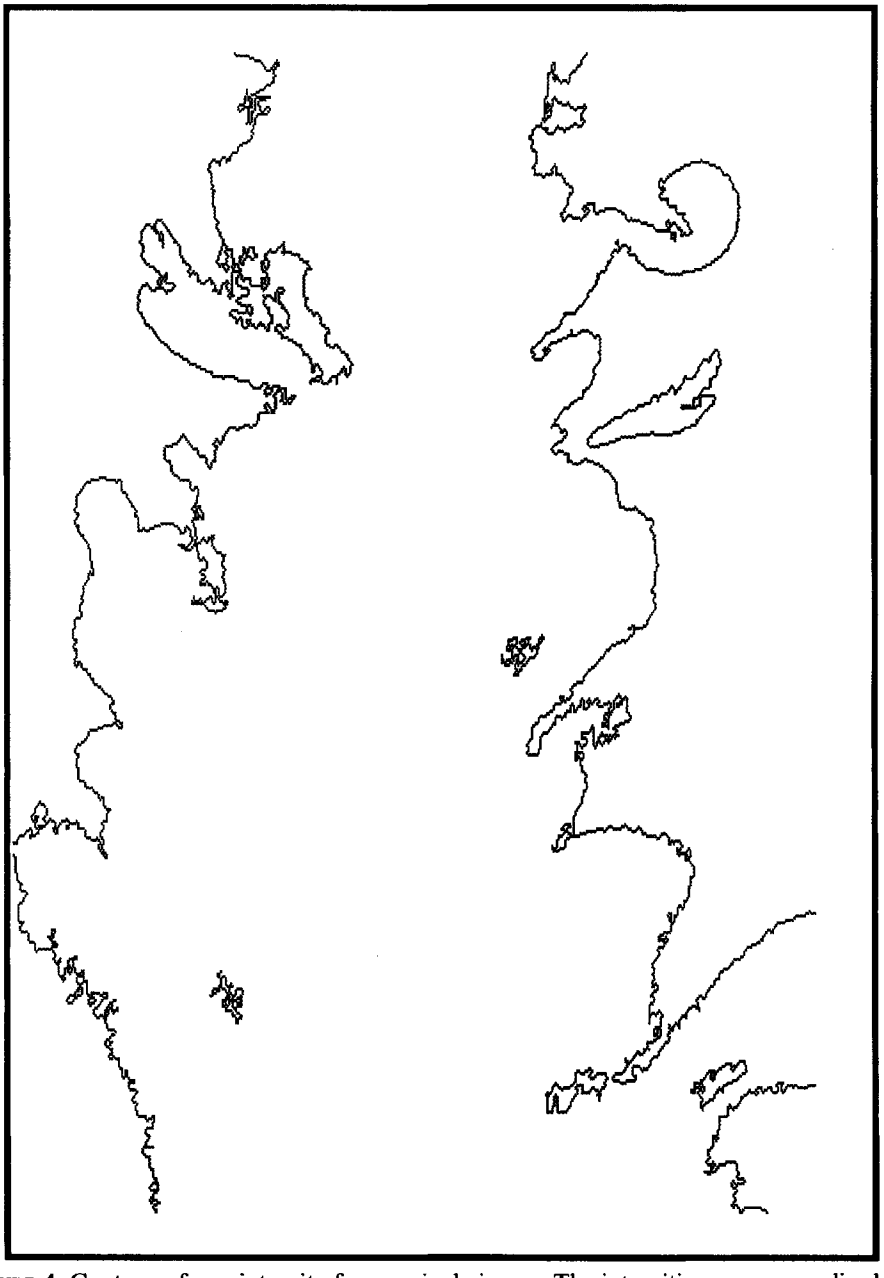

FIGURE 4. Contour of one intensity from a single image. The intensities were normalized with respect to the centreline mean before contouring.

second). The mean values along the centreline of each jet or plume were used to normalize the intensities, so that intensities were normalized by the local mean centreline value.

For each experiment 16 instantaneous images were captured at intervals of about 5 s. The concentrations were normalized by the centreline mean as described above and contours of concentration were found. An example of a contour is given in figure 4. The fractal dimension of such contours was found by a box counting method, with the

intensity threshold for contours in the range 0.1 to 1.1 times the local mean centreline value. Because the flow spreads with distance from the source it is necessary to use boxes that are related to the local lengthscale (i.e. plume width) as sketched in figure 5. A range of box sizes was used the largest of side equal to approximately half the local plume width, with a ratio of lengths from the largest to smallest of about 100.

4. Results

Mean intensities were calculated as described above. The intensities were then normalized with respect to the centreline mean. This mean was found by averaging the central 25 pixels (5 mm) of the image. Contours of normalized mean intensity are shown in figure 6. Two main differences were found between the mean concentration profiles for jets and plumes. First the jets spread at a wider angle than the plumes, and second the cross-stream profile is different. While the plumes fitted a Gaussian profile the jets did not. Trying profiles of the form $\exp(-|r/r_S|^n)$, it was found that $n \approx 2.6$ gave the best fit for jets (in the sense that if the range of data was varied, a constant value for r_S was obtained). Putting a factor of $((n-1)/n)$ in the exponential, so that the point of inflexion is at $r = \pm r_S$, the results for the mean distribution were: for jets

$$C = C_0 \exp\left\{\left(\frac{-1.6}{2.6}\right)\left(\frac{|r|}{r_S}\right)^{2.6}\right\},$$

with

$$r_S = (0.164 \pm 0.005)\, z;$$

and for plumes

$$C = C_0 \exp\left\{\left(\frac{-1}{2}\right)\left(\frac{|r|}{r_S}\right)^{2}\right\},$$

with

$$r_S = (0.085 \pm 0.005)\, z,$$

where z is the distance from the source (jets) or virtual origin (plumes). Note that for plumes the flow is initially jet-like, with a correspondingly larger spreading angle. The spreading rate given above is determined from distances greater than a jet length with z measured from a virtual origin behind the source. The plume spreading rate is in agreement with that found by Rouse, Yih & Humphreys (1952): they found $r_S = 0.084$. For comparison between jets and plumes, and work by other authors, it is convenient to describe the spreading in terms of the contour of 50% of the mean centreline value. Defining $r_{\frac{1}{2}}$ as the radius at which the mean concentration is half that of the centreline value gives, for jets,

$$r_{\frac{1}{2}} = (0.172 \pm 0.005)\, z,$$

and for plumes,

$$r_{\frac{1}{2}} = (0.100 \pm 0.006)\, z.$$

For each experiment 16 images were used to calculate the fractal dimensions. For each image the dimensions of several contours were calculated. The mean dimension for a given contour intensity was then calculated from the 16 realizations for each experiment. For example, to calculate the dimension of the 30% contour for an experiment the dimension of the 30% contour in each of the 16 images for that experiment was calculated, and then the mean of those 16 values taken. Plots of number of boxes versus box size for four images from one experiment are shown in figure 7; the dimension was found by fitting straight lines to such data using a least-

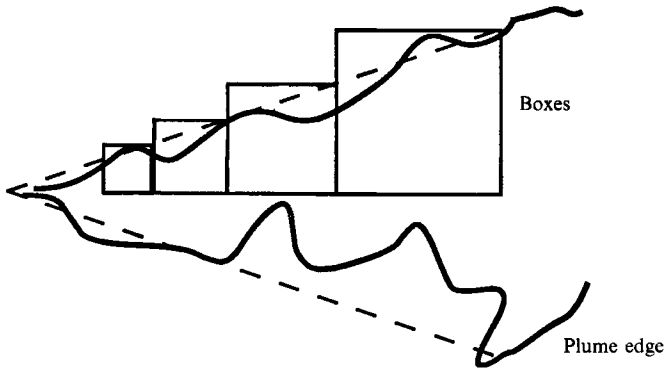

FIGURE 5. Diagram illustrating the box counting method used to determine the dimension of contours.

squares fit. The data are close to a straight line but there is a distinct curve. This is probably due to the small range between the integral and Kolmogorov scales at the Reynolds numbers of these experiments: the largest box-dimension used was close to the integral scale, the smallest box-dimension was only a few times the Kolmogorov scale. The fractal dimension of the contours is different for contours of different intensity as shown in figure 8, though there is little difference between the same contour intensity for different experiments. The high fractal dimension for low concentrations corresponds to the high fractal dimension of the background noise.

A feature of particular interest is the value of the fractal dimension in the flat part of the graph around the minimum, corresponding to the dimension of the line separating the turbulent plume fluid from the ambient fluid. The fractal dimension of this interface was found to be 1.23 for both jets and plumes (the standard deviation of the mean position of the minimum was ± 0.01). No systematic variation of this value with jet length or Reynolds number was found. It was pointed out earlier that the light sheet was much thicker than the Kolmogorov scale, so that the image is effectively a two-dimensional projection of the plume rather than a true two-dimensional cut. The value of 1.23 is in agreement with the value found for jets and clouds by Prasad & Sreenivasan (1990). According to the Prasad & Sreenivasan results for slits of various widths a projection dimension of 1.23 would correspond to a true dimension of 2.37 for the boundary surface. Constantin, Procaccia & Sreenivasan (1991) have shown that the dimension of a contour imbedded in the fully turbulent part of the flow is 2.67 (i.e. larger than that for the boundary), and this might explain the higher measured dimension for contours of higher concentration shown in figure 8, though there are no other results for the projections of surfaces within the fully turbulent region. However, it must be remarked that there is a tendency to undercount the number of big boxes for contours of high concentration as one box will cover the contour on both sides of the plume, giving an overestimate of the dimension for the higher concentrations.

While the graphs shown in figure 8 are fairly flat in the neighbourhood of the minimum it could be argued that the minimum is just an artefact of the particular noise-level cutoff for these experiments. The slopes of the graphs are fairly constant for C/C_0 in the range 0.3 to 0.6, and continuing this slope to the intercept where the concentration is zero gives a value for the dimension of 1.16 (with standard deviation of the intercept of ± 0.02).

(a)

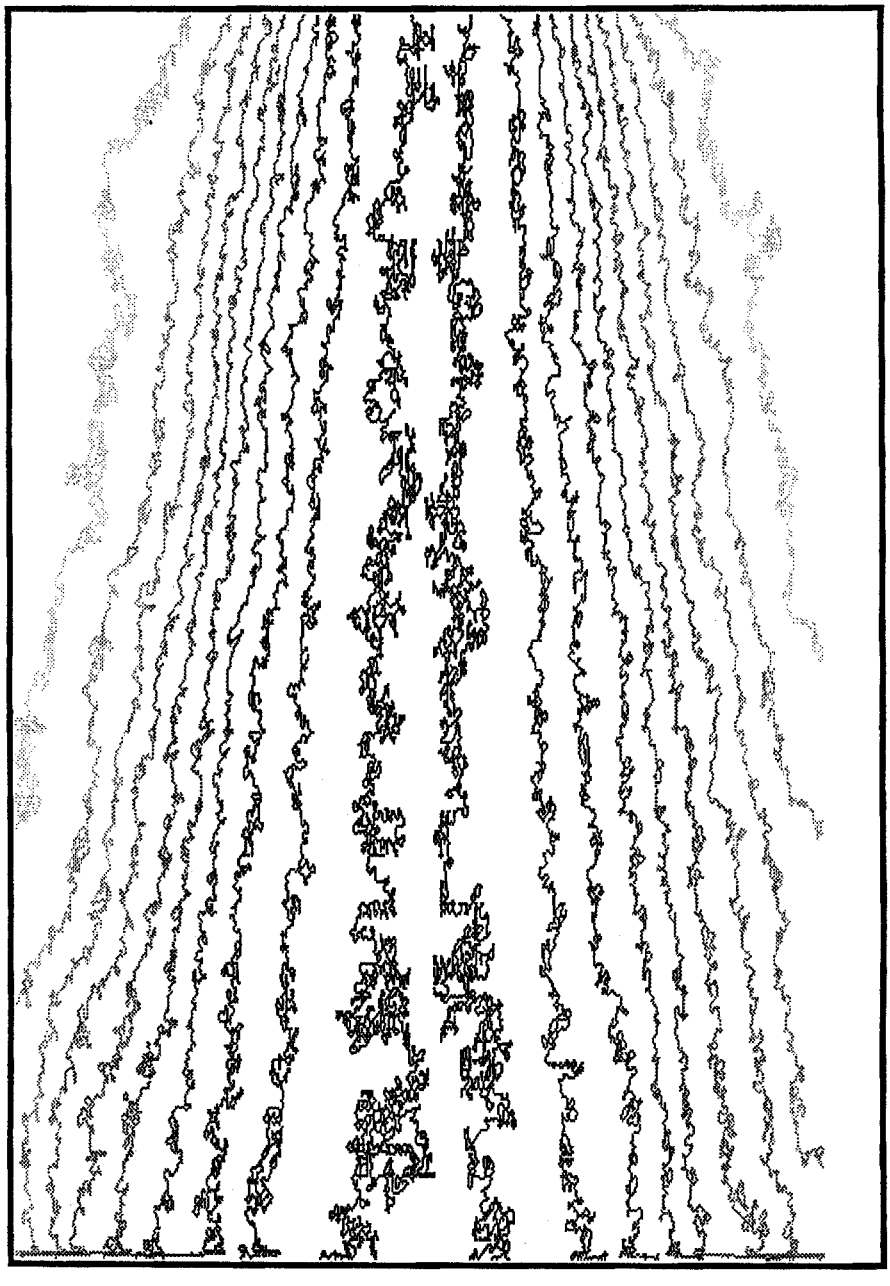

FIGURE 6(a). For caption see facing page.

5. Discussion

The fractal dimensions of concentration contours in jet and plume flows have been measured. In making these measurements careful normalization with respect to the local concentration and length scales has been made. The measured dimensions of the contours were found to be the same for jets and plumes despite the presence of buoyancy forces in the latter case. It should be noted that presuming the flows to be Reynolds-number independent leads to the same value of the fractal dimension

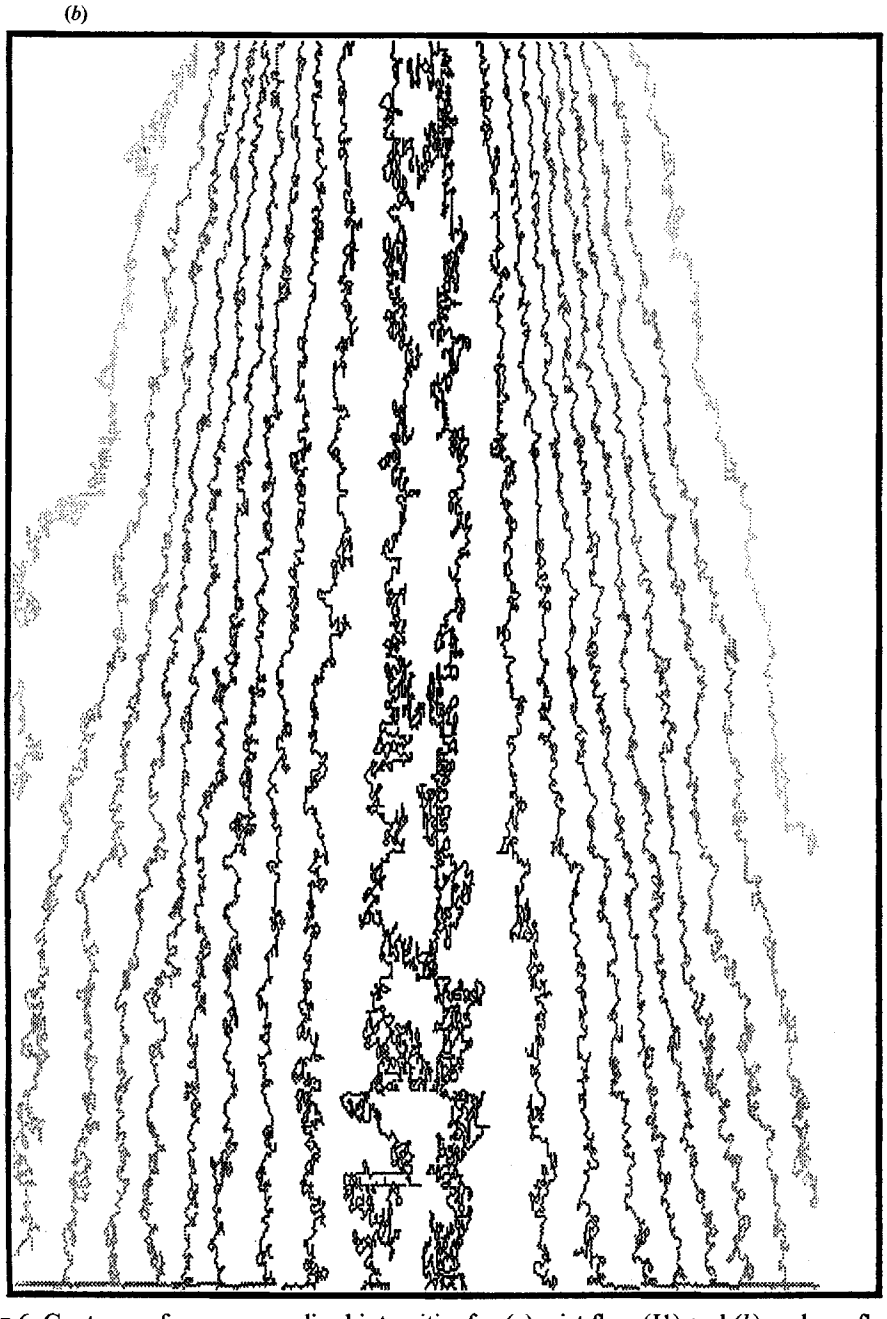

FIGURE 6. Contours of mean normalized intensities for (*a*) a jet flow (J1) and (*b*) a plume flow (P1). Note the wider spreading angle of the jet flow. The contours are at intervals of 10% of the centreline mean.

regardless of the flow type (see, for example, Sreenivasan 1991). This is because the total diffusion (of momentum or scalar tracers) is set by the larger scales and the area at the smallest scale must be of the correct size to allow this diffusion to take place. Thus, whilst buoyancy has an influence upon the large-scale properties of the flow, the small-scale features depend only upon the scales set by the type of flow. Thus the small-

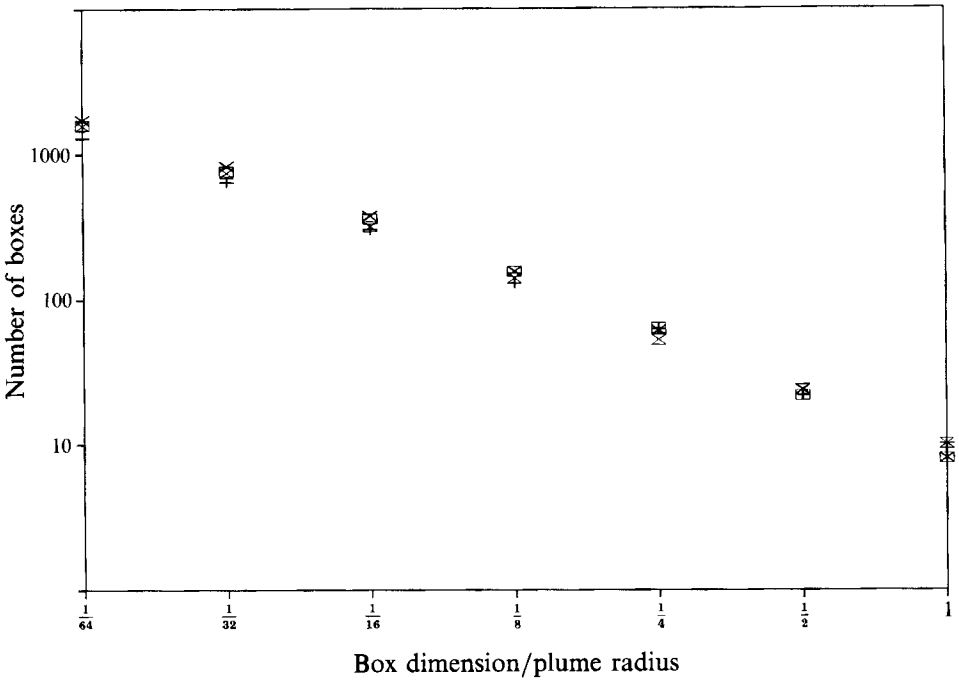

FIGURE 7. Examples of box number versus box size plots. The results are for the 30% contour on four images from one experiment (J1). Different symbols are used for the different images.

scale features are very similar for jets and plumes, with buoyancy having no appreciable direct effect. The larger scales are affected, however, with jets having a broader spread of the mean concentration profiles than plumes and there is also a slight difference in the form of the profile.

There was found to be significant variation of dimension with threshold (see figure 8). The minimum dimension was found to be 1.23, at a threshold of approximately 25% of the local mean, and this is in agreement with previous workers. However, it could be the case that this minimum is just an artefact of the noise-level cutoff in these experiments. The estimated dimension of the zero concentration contour (1.16) may be a more useful quantity, but it is clear that no single value for the dimension gives a complete description.

The significant changes of dimension with threshold raises doubts about the results of earlier authors using contours of constant (un-normalized) concentration. Such contours will follow the outer part of the flow with low values of C/C_0 (and low dimension) in the upstream part of the image, but move into the interior (with higher dimension) further downstream. The measured dimension will be an average weighted towards the downstream part of the flow. This weighting comes from the fact that the contour lengths will be longer downstream, partly because the flow is broader (relative to constant-sized boxes) and partly because the dimension is increased. Sufficiently far downstream, for a given threshold, the contour length will decrease again as there are only small regions with very high concentration. In the present experiments the maximum contour length (for a given box scale) occurs for contours of threshold approximately equal to the local centreline mean (i.e. $C/C_0 \approx 1.0$), and drops off sharply beyond this (which is why no data are presented for $C/C_0 > 1.1$). Furthermore, varying the threshold in un-normalized measurements will tend to result in simply measuring a similar contour further up- or downstream in the image. The result will be

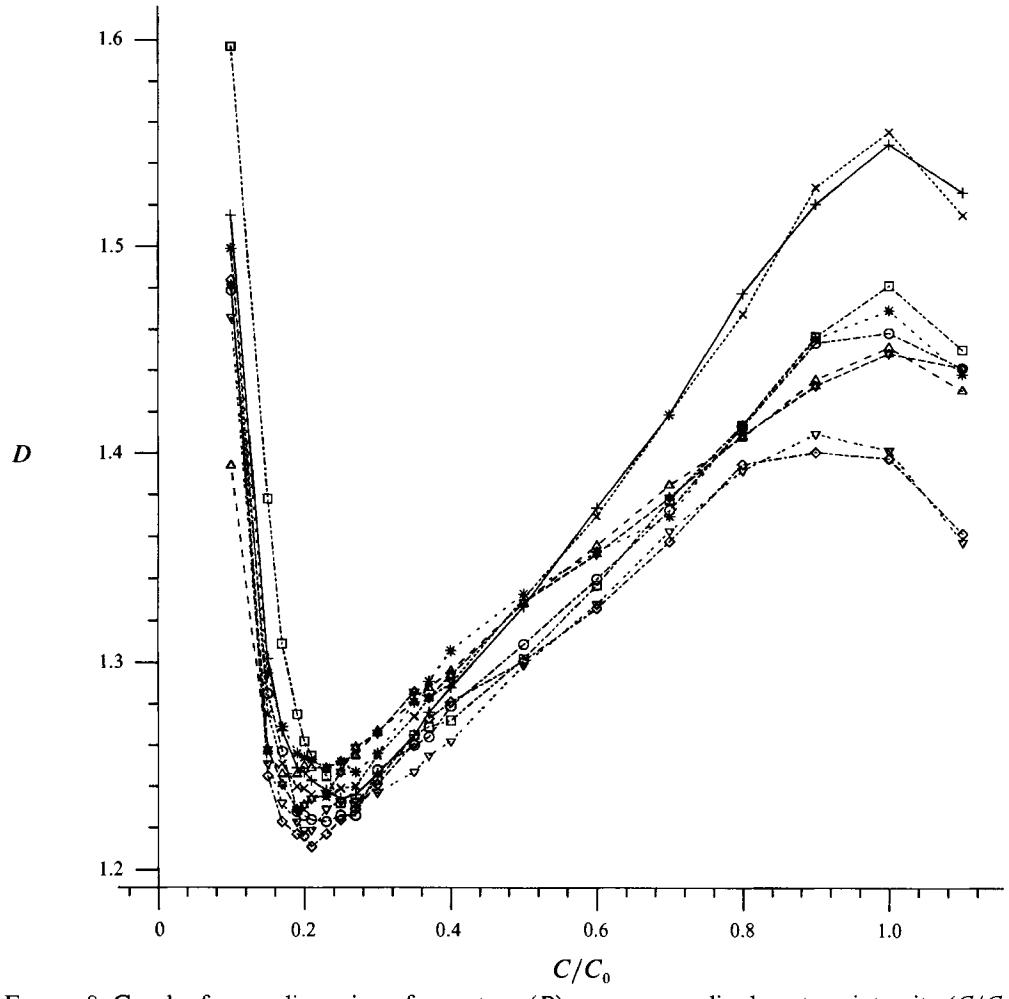

FIGURE 8. Graph of mean dimension of a contour (D) versus normalized contour intensity (C/C_0). Note the minimum dimension at about the 20 to 25% contour in all cases. (Symbols given in table 1.)

that little change in the measured dimension would be observed until the threshold is changed sufficiently so that a significant part of the contour is no longer in the viewed area. This is likely to give a false plateau in dimension versus intensity plots. In short, if there are significant variations in the local scales for concentrations and length then these must be accounted for when examining fractal dimensions.

This study was undertaken whilst I was a Research Fellow at the Department of Applied Mathematics and Theoretical Physics (DAMTP), Cambridge, funded by the Natural Environment Research Council. I would like to thank the technicians at DAMTP for their help with designing and building the apparatus, and the referees for their constructive comments and useful references. I also especially thank Dr S. B. Dalziel, without whose work and advice on image processing this study would not have been possible.

REFERENCES

CONSTANTIN, P., PROCACCIA, I. & SREENIVASAN, K. R. 1991 Fractal geometry of isoscalar surfaces in turbulence: theory and experiments. *Phys. Rev. Lett.* **67**, 1739–1742.

CROW, S. C. & CHAMPAGNE, F. H. 1971 Orderly structure in jet turbulence. *J. Fluid Mech.* **48**, 547–591.

HUNT, J. C. R. & VASSILICOS, J. C. 1991 Kolmogorov's contributions to the physical and geometrical understanding of small-scale turbulence and recent developments. *Proc. R. Soc. Lond.* A **434**, 183–210.

KOTSOVINOS, N. E. 1990 Dissipation of turbulent kinetic energy in buoyant free shear flows. *Intl J. Heat Mass Transfer* **33**, 393–400.

LIST, E. J. 1982 Turbulent jets and plumes. *Ann. Rev. Fluid Mech.* **14**, 189–212.

MORTON, B. R., TAYLOR, G. I. & TURNER, J. S. 1956 Turbulent gravitational convection from maintained and instantaneous sources. *Proc. R. Soc. Lond.* A **234**, 1–23.

PAPANICOLAOU, P. N. & LIST, E. J. 1988 Investigations of round vertical turbulent buoyant jets. *J. Fluid Mech.* **195**, 341–391.

PAPANTONIOU, D. & LIST, E. J. 1989 Large-scale structure in the far field of buoyant jets. *J. Fluid Mech.* **209**, 151–190.

PRASAD, P. R. & SREENIVASAN, K. R. 1990 The measurement and interpretation of fractal dimensions of surfaces in turbulent flows. *Phys. Fluids* A **2**, 792–807.

ROUSE, H., YIH, C.-S. & HUMPHREYS, H. W. 1952 Gravitational convection from a buoyancy source. *Tellus* **4**, 201–210.

SREENIVASAN, K. R. 1991 Fractals and multifractals in fluid turbulence. *Ann. Rev. Fluid Mech.* **23**, 539–600.